NONLINEAR BUCKLING OF COMPRESSED FRP CYLINDRICAL SHELLS

*Seishi Yamada, Member of JSCE, Toyohashi University of Technology, Japan
James G. A. Croll, Fellows of REng and ICE, University College London, UK
Nobuhisa Yamamoto, Graduate Student, Toyohashi University of Technology, Japan

1. INTRODUCTION

The constant demand and necessity for light weight efficient structures have recently led the structural engineer to the field of structural optimization and simultaneously to the use of non-conventional materials, such as fiber reinforced polymeric (FRP) matrix composites, primarily because of their high-strength to weight ratios. There exists a large activity in the area of material characterization, analysis, fabrication and design of composite structures. The lightweight and the high corrosion resistance of FRP composites make them particularly suitable for bridges, aerospace components, storage tanks or large-span structural members. In this paper the FRP structural members that are modeled are thin-walled orthotropic cylindrical shells and it is their elastic buckling criteria under axial compression forces that are considered. It is well-known that axially compressed cylindrical shells have a buckling behavior which is very sensitive to initial geometric imperfections[1). The present paper investigates the non-linear buckling behaviour of the FRP composite cylindrical shell having material properties similar to those of experimentally studied columns previously by the first author. From accurate solutions of the nonlinear shell equations it will be demonstrated that for increasing amplitudes of initial imperfections the elastic buckling loads exhibit well defined lower bounds.

2. ANALYTICAL METHOD

For an imperfect thin-walled circular cylinder of longitudinal length *L*, wall-thickness *t*, and radius *R*, shown in Fig.1, the change in the total potential energy, consequent upon the application of a uniform axial compression stress of σ, may be written as

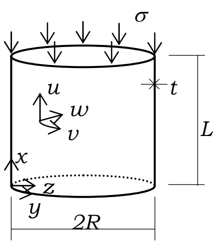

Fig.1 A Cylindrical Shell

$$\Pi = \Pi_M + \Pi_B + \Pi_\lambda \quad (1)$$

$$\Pi_M = \frac{1}{2}\int_0^{2\pi R}\int_0^L \left(n_x\varepsilon_x + n_y\varepsilon_y + 2n_{xy}\varepsilon_{xy}\right)dxdy \quad (2a)$$

$$\Pi_B = \frac{1}{2}\int_0^{2\pi R}\int_0^L \left(m_x\kappa_x + m_y\kappa_y + 2m_{xy}\kappa_{xy}\right)dxdy \quad (2b)$$

$$\Pi_\lambda = \int_0^{2\pi R}\int_0^L \left\{-(-\sigma)t\frac{\partial u}{\partial x}\right\}dxdy \quad (2c)$$

where Π_M is the membrane strain energy, Π_B the bending strain energy, and Π_λ the increase in load potential for an axial compressive stress of σ.

The strain-displacement relations associated with deformation from an initial imperfection, w^0, are taken to be of the Donnell-Mushtari-Vlasov type for shallow shells. The bending and membrane stress resultants are related to strains through the orthotropic constitutive equations

$$m_x = D\left(\mu_{11}\kappa_x + \mu_{12}\kappa_y\right),\ n_x = K\left(\eta_{11}\varepsilon_x + \eta_{12}\varepsilon_y\right) \quad (3)$$

$$m_y = D\left(\mu_{12}\kappa_x + \mu_{22}\kappa_y\right),\ n_y = K\left(\eta_{12}\varepsilon_x + \eta_{22}\varepsilon_y\right) \quad (4)$$

$$m_{xy} = D\mu_{66}\kappa_{xy},\ n_{xy} = K\eta_{66}\varepsilon_{xy} \quad (5)$$

$$D = E_0t^3\Big/\left\{12\left(1-\nu_0^2\right)\right\},\ K = E_0t\Big/\left(1-\nu_0^2\right) \quad (6)$$

where $\nu_0 = 1/3$ and E_0 are basically constants.

The end boundary is assumed to be supported in such a way as to confirm with the classical simple support, corresponding with the conditions

$$w = 0,\ \frac{\partial^2 w}{\partial x^2} = 0,\ \frac{\partial u}{\partial x} = 0,\ v = 0 \quad \text{at} \quad x = 0, L \quad (7)$$

By taking displacement functions *u*, *v* and *w* as linear combinations of the harmonic expressions, these boundary conditions will be exactly satisfied since each separate component satisfies the boundary conditions of Eq (7).

The initial geometric imperfection is expressed as

$$w^0 = w^0{}_{b,1}\cos\left(by/R\right)\sin\left(\pi x/L\right) \quad (8)$$

3. STRUCTURAL MODELLING

The compressive stress may be written in terms of the non-dimensional load parameter λ as

$$\lambda \equiv \sigma/\sigma_{cl},\quad \sigma_{cl} = tE_0\Big/R\sqrt{3(1-\nu_0{}^2)} \quad (9)$$

In this analytical study, a commercially available unidirectional glass fiber laminar unit with a 0.2 mm thickness has been adopted and the forty lamination of the unit has obtained four type orthotropic cylindrical shells with symmetric three-layers and a t = 8mm thickness as listed in Table 1. The basic Young modulus E_0 in Eq.(9) was taken to be 27.1GPa which is the average value of the bending stiffness in x-direction and in y-direction. Total volume of fiber has been adopted to be V = 60%, and the fiber volume ratio in circumferential direction V_y is adopted to be a parameter in this study. Table 2 shows the coefficients in Eqs (3)-(5) obtained from the classical lamination theory.

Key Words: cylindrical shell, fiber reinforced polymer, axial compression, buckling, imperfection
Address: Tempaku-cho, Toyohashi 441-8580, Japan. Tel:0532-44-6849, Fax:0532-44-6831

Table 1　Lamination Details

model	V_y/V	fiber orientation angle(deg.)	90	0	90
C20T	0.2	number of lamina	4	32	4
C50T	0.5		10	20	10
C80T	0.8		16	8	16
model	V_y/V	fiber orientation angle(deg.)	0	90	0
C50L	0.5	number of lamina	10	20	10

Table 2　Coefficients in Eqs (3)-(5)

	η_{11}	η_{12}	η_{22}	η_{66}	μ_{11}	μ_{12}	μ_{22}	μ_{66}
C20T	1.261	0.061	0.510	0.193	0.909	0.044	0.879	0.193
C50T	0.896	0.061	0.896	0.193	0.415	0.028	1.371	0.193
C80T	0.513	0.062	1.285	0.194	0.265	0.032	1.523	0.194
C50L	0.896	0.061	0.896	0.193	1.371	0.094	0.415	0.193

4. RESULTS AND DISCUSSIONS

In this paper the results of $Z=\sqrt{1-\nu_0{}^2}\,L^2/(Rt)=100$ are shown in figures due to the limit of space. It has been well-known that the geometrical parameter of the complete cylinders is only this Batdorf parameter Z when the shallow shell assumption (DMV-formulation) is used. That is, all governing equations can be normalized using only the independent geometric parameter Z. But in non-linear numerical step-by-step calculation another geometric parameter is needed to be defined. In the present study, the radius thickness ratio R/t has been selected, and then referring to previous papers[1,2] $R/t = 405$ was adopted.

Included in Fig.2 are representative imperfect curves for C50T (b=11), where the horizontal axis represents the total displacement component having circumferential wave number b and the single axial wave number. It can be seen that the sensitivity of buckling load to changes in imperfection is most severe when the imperfection has a very small amplitude.

Selected nonlinear-analytical obtained buckling loads λ^c are plotted in Fig.3 for various imperfection amplitudes and circumferential wave number of imperfection b. The maximum buckling loads $\lambda^c_{\max}$ for perfect (imperfection free) shells are much sensitive to the ratio V_y/V as well as the lamination detail in Table 1, however, the lower limit for large imperfections has almost the same circumferential wave $b=9\sim11$. The minimum buckling loads $\lambda^c_{\min}$ on each figure in Fig.3(a)-(d) are listed in Table 3 which shows $\lambda^c_{\min}$ decreases as the ratio V_y/V increases.

Table 3　Minimum Buckling Loads

	$\lambda^c_{\min}$	b	$w^0_{b,1}/t$
C20T	0.1661	11	1.20
C50T	0.1586	11	1.40
C80T	0.1330	9	2.00
C50L	0.1539	11	1.00

Figure 4 shows the imperfection sensitivity, where the vertical axis is the ratio $\lambda^c/\lambda^c_{\max}$. You can see that in all the cases the lower bounds of $\lambda^c/\lambda^c_{\max}$ are approximately equal to 0.3, however, the case of C50L has much more sensitive to the case of C50T. These characteristics are obtained in other cases for various wave number b.

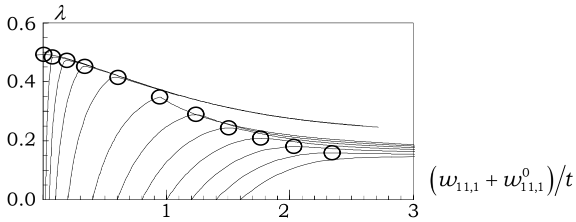

Fig.2　Load versus Deflection Curves for C50T(b=11)

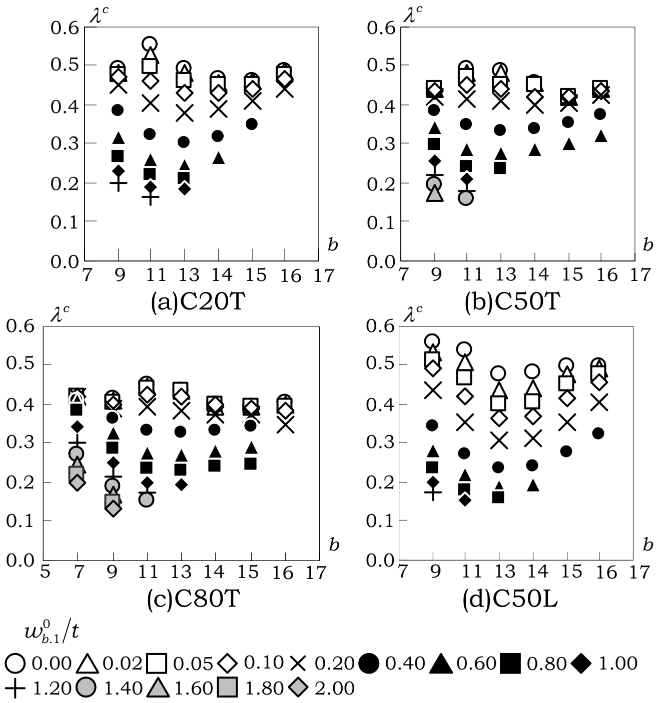

Fig.3　Non-Linear Buckling Loads

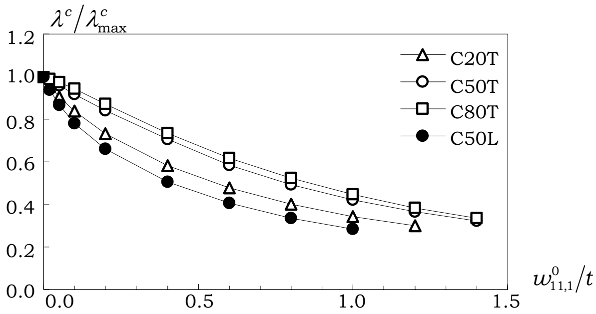

Fig.4　Initial Imperfection Sensitivity

REFERECES

1) Yamaki, N.: *Elastic Stability of Circular Cylindrical Shells*, North-Holland, 1984.

2) Yamada, S. and Croll, J.G.A.: Contributions to understanding the behavior of axially compressed cylinders, *Journal of Applied Mechanics*, ASME, Vol.66, pp.299-309, 1999.